

## Determination of the ray surface and recovery of elastic constants of anisotropic elastic media: a direct and inverse approach

This article has been downloaded from IOPscience. Please scroll down to see the full text article.

1995 J. Phys.: Condens. Matter 7 3863

(<http://iopscience.iop.org/0953-8984/7/20/007>)

View [the table of contents for this issue](#), or go to the [journal homepage](#) for more

Download details:

IP Address: 171.66.16.151

The article was downloaded on 12/05/2010 at 21:18

Please note that [terms and conditions apply](#).

# Determination of the ray surface and recovery of elastic constants of anisotropic elastic media: a direct and inverse approach

Litian Wang

Department of Physics, University of Oslo, PO Box 1048, Blindern, 0316 Oslo, Norway and Hedmark College, 2450 Rena, Norway

Received 3 May 1994, in final form 20 February 1995

**Abstract.** Propagation of plane acoustic waves in anisotropic media can be characterized by the slowness surface and ray surface which represent phase velocities and group velocities, respectively. The mathematical expressions for the slowness surface in terms of elastic constants are well established and provide a foundation for acoustic determination of the elastic constants of anisotropic elastic media. However, a direct mathematical formulation of the ray surface has not been fully developed because of the many-to-one correspondence between the ray surface and the slowness surface. Based upon the Stroh formalism for two-dimensional elastodynamic systems, we establish in this paper a direct and analytical formalism, the degeneracy analysis approach (DAA), for the construction of the ray surface and the recovery of elastic constants for anisotropic media. A special emphasis is put on the group velocities along symmetry directions with respect to symmetry planes, for which an explicit expression for the group velocity is given in terms of the elastic constants so that the inverse problem can be solved easily. Particularly, the complication of cuspidal points due to the presence of axial concavity in the slowness surface is treated and it is apparent that the presence of a cuspidal point becomes an advantage for the inverse problem of recovery of elastic constants.

## 1. Introduction

The determination of elastic constants of anisotropic media from acoustic wave experiments is usually based on the phase velocity measurement. The main reason for this is that there exist straightforward and explicit analytical relations between the elastic constants and the phase velocity  $c$  or the slowness  $s = c^{-1}$  which determines a slowness surface  $s(\mathbf{k}) = c^{-1}(\mathbf{k})\mathbf{k}$ , where  $\mathbf{k}$  is the unit wave-vector. In contrast, the group velocity is seldom used for such a purpose because the theoretical investigations of the group velocity  $v_g$  have not been able to provide a practical and direct formulation for the relation between the elastic constants and the group velocity  $v_g$  which determines the ray surface  $r(\mathbf{g}) = v_g(\mathbf{g})\mathbf{g}$  or inverse ray surface  $v_g^{-1}(\mathbf{g})\mathbf{g}$ , where  $\mathbf{g}$  is the unit ray-vector [1, 2].

Basically, for a bulk wave with the wave-vector  $\mathbf{k}$  and the phase velocity  $c$ , its associated ray-vector  $\mathbf{g}$  and group velocity  $v_g$  are not necessarily identical to  $\mathbf{k}$  and  $c$  respectively. Instead, there exist relations  $v_g = c / \cos \hat{\phi}$  and  $\hat{\phi} = \cos^{-1}(\mathbf{g} \cdot \mathbf{k})$ , where  $\hat{\phi}$  is the inclination angle of the wave-vector  $\mathbf{k}$  from the ray-vector  $\mathbf{g}$ . Such a difference between the slowness surface and the ray surface leads to distinction between direct and inverse problems based on phase velocity measurements and based on group velocity measurements.

The direct and inverse problem for phase velocity measurements is well established. The analytical solution of the Christoffel equation makes the direct approach very simple, i.e., given the elastic constants, the Christoffel equation will yield three sheets of slowness surface where the phase velocity is expressed explicitly as a function of the wave-vector  $k$ ; the density  $\rho$  will enter only as a simple scaling factor. The inverse problem has also been studied extensively in connection with recovering elastic constants from phase velocity measurements. So far, the best inverse approach suggested can determine not only the elastic constants but also the crystallographic orientation of samples [3, 4].

However, the direct and inverse problems for the ray surface in connection with group velocity measurements have not been developed to the same extent. A little has been achieved developing straightforward direct and inverse formulations for the group velocity and the ray surface, that is, given the elastic constants, the group velocity is derived as a function of ray-vector  $g$ , and conversely, given group velocity for any direction  $g$  the elastic constants can be recovered. Up to now, even the direct formulation has been addressed in a rather indirect fashion: for given elastic constants, the ray surface (group velocity) is *indirectly* deduced from the slowness surface (phase velocity) in terms of parametric equations of the wave-vector  $k$ , instead of in terms of the ray-vector  $g$  [1, 2]. This is inconvenient when it comes to solving the inverse problem.

There are many difficulties in deriving straightforward direct and inverse formulations related to the ray surface. The ray surface has a high number of degrees of freedom, up to 150, while the slowness surface has only six. This is so because of the generic relation between the two surfaces which is polar reciprocal. According to the theory of characteristics for hyperbolic differential equations, the inverse ray surface  $v_g^{-1}(g)g$ , as a bicharacteristic surface of the Christoffel equation, is the pedal of the slowness surface [1]. We notice that the term pedal implies that dimensionality is involved in the construction of the ray surface [5]. In the two-dimensional case the pedal can be associated with the tangent line over a slowness curve [1], while in the three-dimensional case the pedal is related to the tangent plane over the slowness surface [1, 6]. In this sense, we need to make a distinction between the *ray surface* for the three-dimensional case and the *ray curve* for the two-dimensional case. Terminologically, the term ray surface refers to the ray curve when the dimensionality consideration is obvious. In this paper, we will use the term ray surface to refer to the ray curve in the two-dimensional case throughout our discussion except for cases mentioned explicitly. The term slowness surface is also used for the description of the slowness curves as used in most of the literature.

Even for two-dimensional cases, the presence of concavities in the slowness surface will cause the ray surface to be multivalued. Such a one-to-many correspondence between the slowness surface and the ray surface, is a major obstacle for the many attempts to discuss the direct problem analytically and it also complicates the inverse problem. Many studies have resorted to other alternatives. Recently, measurements of group velocities using the so-called point source/point receiver method have been reported [7, 8, 9] and the recovery of elastic constants has been carried out using selected group velocity measurements and optimization methods [10] which are very sensitive to selected values of the elastic constants.

In this paper, we intend to solve both the direct and the inverse problems regarding the ray surface and recovery of elastic constants from group velocity measurements in two-dimensional cases (line source) and to make the methods applicable to three-dimensional cases (point source) also. The essential physical and mathematical basis is the Stroh eigenvalue formalism and degeneracy analysis of the pedal construction. In section 2 we will briefly review the Stroh formalism and its relation to the slowness surface and the inverse ray surface, and provide a general direct approach for analytical and numerical calculation

of the group velocity and the ray surface. Such a general approach has the advantage that it allows one to obtain the group velocity  $v_g$  as well as the inclination angle  $\hat{\phi}$ , and it can also provide a scheme for recovering the slowness surface by the pedal construction applied to the ray surface [1]. In section 3, we will present explicit analytical formulations for group velocity in some symmetry directions with respect to symmetry planes, from which solutions for the inverse problem follow immediately. Emphasis is put on the discussion of group velocities for pure modes and cuspidal points. It turns out that the presence of a cuspidal point becomes an important advantage for the purpose of recovering elastic constants. For the cases where the ray-vector directs along off-symmetry directions, we implement the degeneracy analysis numerically, which enables us to recover all the elastic constants even when there is no concavity in the slowness surface or when the concavity is centred along the off-symmetry direction with respect to the symmetry plane.

## 2. The degenerate Stroh formalism and group velocity

Let us first ask, for a given ray direction, say a unit ray-vector  $g$ , what is the group (ray) velocity  $v_g$  along this direction and what is the phase velocity  $v$  of the corresponding plane wave? For the plane wave solution in two-dimensional systems, it is known that the unit wave-vector  $k$  of a plane wave would have an inclination angle  $\hat{\phi}$  from the direction  $g$ , and the phase velocity  $c$  and the group velocity  $v_g$  obey the relation  $c = v_g \cos \hat{\phi}$ . In a two-dimensional system, we can define two mutually orthogonal unit vectors,  $m$  and  $n$ , with  $m$  parallel to  $g$ , so that the wave-vector  $k$  for the bulk plane waves can be expressed by  $k = \cos \hat{\phi} m + \sin \hat{\phi} n$ , and  $k \cdot g = \cos \hat{\phi}$ , where the angle  $\hat{\phi}$  is the inclination angle. We will show later that  $\hat{\phi}$  is a special value associated with the degeneracy of the Stroh eigenvalue problem and, only under such a degenerate case, the unit ray-vector  $g$  and the vector  $m$  are parallel and  $\hat{\phi}$  represents the inclination angle.

### 2.1. Standard Stroh formalism [11, 12]

In a general sense, we will consider a wave with the wave-vector  $k = m + pn$  with a displacement field described by

$$u(x, t) = A \exp[i k(m \cdot x + pn \cdot x - vt)] \quad (2.1)$$

where  $k$  and  $v$  are the wave-number and the velocity, and  $A$  is the polarization vector. Generally, we take  $p$  as a complex number. Clearly, when  $p$  is real, (2.1) describes a bulk (homogeneous) wave propagating along  $k$ , and when  $p$  is a complex number it represents an inhomogeneous wave whose amplitude will attenuate or amplify exponentially with distance normal to the plane  $n \cdot x = 0$ , depending on the sign of  $\text{Im } p$ . We denote the space spanned by  $m$  and  $n$  as the *reference plane*.

Substitution of (2.1) into the equation of motion

$$C_{ijkl} \frac{\partial^2 u_k}{\partial x_j \partial x_l} = \rho \frac{\partial^2 u_i}{\partial t^2} \quad (2.2)$$

will lead to

$$\mathbf{Q}(kk)\mathbf{A} = \{(mm) + p[(mn) + (nm)] + p^2(nn)\}\mathbf{A} = \rho v^2 \mathbf{A} \quad (2.3)$$

where the  $(mn)$  etc are matrices whose components are defined as  $(mn)_{jk} = m_j C_{ijkl} n_l$ , etc.

The solutions for (2.3) are determined from the characteristic equation

$$R = \|(mm) + p[(mn) + (nm)] + p^2(nn) - \rho v^2 \mathbf{I}\| = 0 \quad (2.4)$$

which is a sixth-order equation in  $p$  and it will yield six complex roots  $p_\alpha, \alpha = 1, \dots, 6$ , which, for sufficiently small value of  $v$  (or lower than slowest bulk wave velocity  $\hat{v}$ ), appear in three complex conjugate pairs. When we increase the velocity  $v$ , a certain pair of the eigenvalues will turn real. For example, the pair  $p_1$  and  $p_2$  for  $v < \hat{v}$ , where  $p_2 = p_1^*$ , will become real roots  $p_1 = \tan \phi_1$  and  $p_2 = \tan \phi_2$  respectively with increasing velocity to  $v > \hat{v}$ .

The solution for a real eigenvalue has a straightforward geometrical interpretation as shown in figure 1(a) (line L), that is, the real eigenvalues are tangents of the angles from the direction  $m$  for two bulk waves along  $k_{1,2} = \cos \phi_{1,2}m + \sin \phi_{1,2}n$ , and their phase velocities are given by  $c_{1,2} = v / \cos \phi_{1,2}$  according to (2.1). Their ray-vectors will be directed along the normal of the slowness surface and have components along both  $m$  and  $n$ .

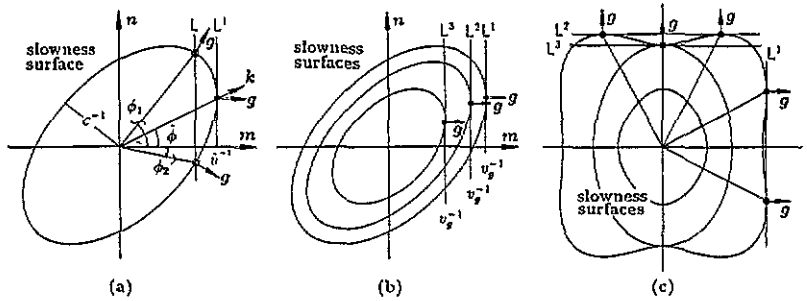


Figure 1. Geometric interpretation of the Stroh eigenvalues and slowness surfaces and their relations to phase velocity and group velocity: (a) bulk wave solutions associated with  $v^{-1}$  marked by the line L whose ray-vectors are parallel to the normal of the slowness surface, and the degenerate solution with  $\hat{\phi}$  at  $\hat{v}^{-1}$  gives the group velocity  $v_g = \hat{v}$  for the wave with  $k$  at an inclination angle  $\hat{\phi}$  from ray-vector  $g$ ; (b) pedal construction for three successive group velocities related to the ray direction  $m$  or  $g$ ; (c) two cuspidal points (C) associated with the double tangent lines  $L^1$  and  $L^2$  with respect to ray directions normal to  $L^{1,2}$  respectively and a tangential acoustic axis along the vertical axis ( $L^3$ ).

In non-dissipative elastic media, the direction of the ray-vector  $g$  is aligned along the energy flux. To study the energy flux, we have to consider the traction vectors associated with the bulk wave solutions from (2.4). It is easy to show that the traction vector  $L_\alpha$  in the plane  $n \cdot x = 0$  associated with the displacement  $A_\alpha$  can then be expressed as

$$L_\alpha = -[(nm) + p_\alpha(nn)]A_\alpha \tag{2.5}$$

and thus the component of the energy flux along the  $n$  direction  $j_n$  is proportional to  $A_\alpha \cdot L_\alpha$ . If a special real eigenvalue is such that  $\hat{p} = \tan \hat{\phi}$  then  $j_n \sim A_\alpha \cdot L_\alpha = 0$ , and  $j$  and  $g$  will be parallel to  $m$ .

Stroh [11] introduced a six-dimensional eigenvalue problem by defining six-dimensional eigenvectors  $\xi_\alpha = (A_\alpha, L_\alpha)^T$  and reformulated equations (2.3) and (2.5) into a standard eigenvalue problem,

$$-\begin{pmatrix} (nn)^{-1}(nm) & (nn)^{-1} \\ (mn)(nn)^{-1}(nm) - (mm) + \rho v^2 \mathbf{I} & (mn)(nn)^{-1} \end{pmatrix} \begin{pmatrix} A_\alpha \\ L_\alpha \end{pmatrix} = p_\alpha \begin{pmatrix} A_\alpha \\ L_\alpha \end{pmatrix}. \tag{2.6}$$

When there is no degeneracy in the eigenvalue problem (2.6), the Stroh eigenvectors fulfil the orthogonality relation

$$A_\alpha \cdot L_\beta + L_\alpha \cdot A_\beta = \delta_{\alpha\beta} \quad \text{for } \alpha = 1, \dots, 6. \tag{2.7}$$

and when non-semisimple degeneracy occurs in a complex conjugate pair or in a real pair, say  $p_\alpha = p_\beta = \hat{p}$  real, where  $\hat{p} = \tan \hat{\phi}$ , and  $A_\beta \rightarrow A_\alpha$ ,  $L_\beta \rightarrow L_\alpha$  and as  $p_\beta \rightarrow p_\alpha$ , the orthogonality relation (2.7) gives

$$A_\alpha \cdot L_\alpha = 0. \quad (2.8)$$

Thus we see that the situation  $A_\alpha \cdot L_\alpha = 0$  is just a degeneracy  $\hat{p} = \tan \hat{\phi}$  in the Stroh eigenvalue equation (2.6), and the wave with  $k = \cos \hat{\phi} m + \sin \hat{\phi} n$  will have its energy flux or ray-vector  $g$  parallel to  $m$ . This is just the case illustrated by the line  $L^1$  in figure 1(a).

The Stroh eigenvalues, unlike the eigenvalues of the Christoffel equation, can be complex. For a given velocity  $v$ , not all the Stroh eigenvalues are necessarily real. The eigenvalues can only become real when the vertical lines, like those in figure 1, have intersected the slowness surface. The number of real eigenvalues is the same as the number of intersections. The remaining eigenvalues will be complex. When a line touches the slowness surface tangentially, the real eigenvalue is duplicate degenerate.

## 2.2. Group velocity

The degeneracy point  $p_\alpha = p_\beta = \hat{p}$  and its associated self-orthogonality (2.8) is a pivotal point in the discussion of group velocity. At such a degeneracy point,  $\hat{v}^{-1} = v_g^{-1}$  implies that the energy flux component  $j_n$  associated with the bulk wave with wave-vector  $k = \cos \hat{\phi} m + \sin \hat{\phi} n$  vanishes and  $g$  is directed along  $m$ , and thus the velocity  $v$  is the group velocity  $v_g$  for the bulk wave and the real eigenvalue  $\hat{p} = \tan \hat{\phi}$  determines the inclination angle  $\hat{\phi}$  between wave-vector  $k$  and the ray-vector  $g$  which is parallel to  $m$  when the degeneracy occurs. In other words, the group velocity is associated with a degeneracy (real number) of the Stroh eigenvalue equation.

Geometrically, the group velocities can be interpreted in the following way. Consider a slowness plot of the three slowness surfaces with respect to the reference plane  $(m, n)$ , and draw a series of vertical tangent lines (see  $L^{1,2,3}$  in figure 1(b)) parallel to  $n$  whose position is marked by  $v_g^{-1}$ . This is exactly a pedal construction. For every single tangent point, the two Stroh eigenvalues, say,  $p_1 = \tan \phi_1$  and  $p_2 = \tan \phi_2$  for the two bulk waves in figure 1(a), have approached the same value  $\hat{p} = \tan \hat{\phi}$  at  $v_g^{-1}$  and  $v_g^{-1} = c^{-1} \cos \hat{\phi}$ .

Note that the degeneracy in the above case is of multiplicity two. In the Stroh formalism, the eigenvalues can degenerate up to multiplicity six [12]. This implies that the group velocity may have a multivalued relation to the geometry of the slowness surface, as illustrated in figure 1(c), where there are two bulk waves with same group velocity.

One typical case, frequently encountered, is the group velocity related to a concavity of the slowness surface where a double-tangent construction as illustrated by the lines  $L^1$  and  $L^2$  in figure 1(c) implies that there are two degeneracies which occur simultaneously, i.e.  $p_1 = p_2 = \tan \hat{\phi}$  and  $p_3 = p_4 = -\tan \hat{\phi}$ . The group velocity for such a case appears in the ray surface as a cuspidal point C. The neighbouring configuration of the concavity will result in a cusp in the ray surface, and the tip of the cusp is related to a triply degenerate Stroh eigenvalue.

Another case is the group velocity associated with a tangential acoustic axis [13]. The tangential acoustic axis is the direction along which two slowness surfaces coalesce tangentially. Along the acoustic axis, as shown by the line  $L^3$  in figure 1(c), the Stroh eigenvalue will be degenerate with multiplicity four,  $p_1 = p_2 = p_3 = p_4 = 0$ .

### 2.3. Ray surface and slowness surface

In the Stroh formalism, the ray surface and the slowness surface are interconnected.

For any given ray direction  $\mathbf{m}$ , every solution for  $v$  related to real eigenvalues  $p = \tan \phi$  will define a bulk wave with phase velocity  $c = v \cos \phi$  and its wave-vector  $\mathbf{k} = \cos \phi \mathbf{m} + \sin \phi \mathbf{n}$ . Therefore, the slowness surface can be constructed by solving the Stroh eigenvalue equation under a single reference orthogonal dyad  $(\mathbf{m}, \mathbf{n})$ .

In order to construct a ray surface, one has to vary the velocity term  $\rho v^2$  in the Stroh eigenvalue equation (2.3), and to trace the group velocities associated with degeneracies (i.e., pedal constructions) for all ray directions, i.e., for all vectors  $\mathbf{m}$ .

This completes the discussion of the analytical scheme for calculation of the ray surface and the slowness surface based on the Stroh formalism. It is shown that the Stroh formalism can be used to derive the group velocity and ray surface in a direct way. The solution of the Stroh eigenvalue problem can give both group velocity and inclination angle, and it enables us to obtain the slowness surface in an alternative way from that based on the Christoffel eigenvalue equation.

One should notice that the non-semisimple degeneracy of the Stroh eigenvalue equation is different from the semisimple degeneracy in the Christoffel equation. In the Christoffel equation, a semisimple degeneracy suggests a so-called acoustic axis around which the polarization vectors are discontinuous. However, the eigenvectors near a non-semisimple degeneracy in the Stroh equation will remain continuous. This is an important distinction between the two equations.

It should be acknowledged that, in two-dimensional systems, the ray surface and the group velocities related to the outer slowness sheet (surface) have been discussed in terms of the transonic states in surface wave theory [12], where many analytical and numerical calculations have been performed for a wide range of cubic and transversely isotropic media [14, 15, 16, 17].

### 3. Group velocity in symmetry planes: the degeneracy analysis approach (DAA)

In the preceding section, we outlined the physical and mathematical basis for the determination of group velocity with respect to the reference plane  $(\mathbf{m}, \mathbf{n})$  in terms of the Stroh eigenvalue formulation. We now substantiate this idea and establish some concrete relations between the group velocity and the elastic constants in anisotropic media. We concentrate on group velocities related to various configurations of the ray surface in some typical symmetry planes of orthotropic media where explicit analytical results can be reached. We first construct a Cartesian coordinate system  $(\mathbf{e}_x, \mathbf{e}_y, \mathbf{e}_z)$  which is coincident with the orthorhombic crystallographic basis [100], [010], [001] and we focus on the group velocities in the (100) plane of orthotropic media; results for other symmetry planes can be readily obtained in a similar fashion.

It is well known that in symmetry planes the slowness surfaces can be described by an elliptic sheet and two non-elliptic sheets [1, 2]. The elliptic sheet represents the out-of-plane (purely transverse) polarized waves and the non-elliptic sheets describe the in-plane polarized waves. In other words, the eigenspace for the Christoffel and the Stroh eigenvalue equations decomposes into a one-dimensional out-of-plane subspace and a two-dimensional in-plane subspace with respect to the symmetry plane [17, 18]. This makes it possible for us to derive some explicit expressions for the group velocities in symmetry planes. As for the group velocity, we adopt the term pure mode to characterize a bulk wave whose phase velocity and group velocity are identical in direction as well as in magnitude.

### 3.1. General formulation for orthotropic media: (100) plane

For the (100) plane in orthotropic media, defining  $m = \cos \varphi e_z + \sin \varphi e_y$ ,  $n = \sin \varphi e_z - \cos \varphi e_y$ , as shown in figure 2 where the direction [001] or  $e_z$  is associated with  $\varphi = 0^\circ$ , we get from (2.3),

$$\mathbf{Q} = \begin{pmatrix} Q_1 & 0 & 0 \\ 0 & Q_2 & Q_4 \\ 0 & Q_4 & Q_3 \end{pmatrix} \quad (3.1)$$

where

$$Q_1 = (c_{55} \cos^2 \varphi + c_{66} \sin^2 \varphi) + (2\Delta_{56} \cos \varphi \sin \varphi)p + (c_{66} \cos^2 \varphi + c_{55} \sin^2 \varphi)p^2 \quad (3.2a)$$

$$Q_2 = (c_{44} \cos^2 \varphi + c_{22} \sin^2 \varphi) + (2\Delta_{42} \cos \varphi \sin \varphi)p + (c_{22} \cos^2 \varphi + c_{44} \sin^2 \varphi)p^2 \quad (3.2b)$$

$$Q_3 = (c_{33} \cos^2 \varphi + c_{44} \sin^2 \varphi) + (2\Delta_{34} \cos \varphi \sin \varphi)p + (c_{44} \cos^2 \varphi + c_{33} \sin^2 \varphi)p^2 \quad (3.2c)$$

$$Q_4 = d_1 \cos \varphi \sin \varphi + d_1 (\sin^2 \varphi - \cos^2 \varphi)p - d_1 (\cos \varphi \sin \varphi)p^2. \quad (3.2d)$$

Here  $d_1 = c_{44} + c_{23}$  and  $\Delta_{kl} = c_{kk} - c_{ll}$ . In orthotropic media, there are nine independent elastic constants, but only a limited number of independent elastic constants are involved in the (100) plane: five diagonal elements and one off-diagonal element, denoted as  $c_{\sigma\sigma}$  and  $c_{\sigma\delta}$  respectively. Thus, the corresponding characteristic equation (2.4) becomes

$$R(p, v, \varphi) = \det(\mathbf{Q} - \rho v^2 \mathbf{I}) = F_1(p, v, \varphi) F_2(p, v, \varphi) = 0 \quad (3.3a)$$

$$F_1(p, v, \varphi) = Q_1(p, \varphi) - \rho v^2 = 0 \quad (3.3b)$$

$$F_2(p, v, \varphi) = [Q_2(p, \varphi) - \rho v^2][Q_3(p, \varphi) - \rho v^2] - Q_4^2(p, \varphi) = 0. \quad (3.3c)$$

It is obvious that, with respect to the reference plane ( $m, n$ ), the eigenspace for the Stroh eigenvalue equation is decomposed into an out-of-plane part and an in-plane part, and that  $F_1$  is related to transversely (out-of-plane) polarized waves belonging to the elliptic (slowness) sheet while  $F_2$  is related to in-plane polarized waves belonging to the two non-elliptic (slowness) sheets [15]. According to the analysis in the previous section, the group velocities ( $v_g$ ) can be determined from (3.3b) and (3.3c) in relation to the degenerate eigenvalues  $p$  for a given direction  $\varphi$ .

**3.1.1. Group velocity related to the out-of-plane elliptic sheet.** We first consider the transversely polarized elliptic sheet shown as the middle slowness surface in figure 2(a). From (3.3b), setting  $F_1(p, v, \varphi) = ap^2 + bp + c = 0$ , we have a pair of Stroh eigenvalues

$$p = [-b \pm (b^2 - 4ac)^{1/2}]/(2a) \quad (3.4)$$

and degeneracy is only possible when  $b^2 - 4ac = 0$ , i.e.,

$$\rho v_g^2 = c_{55}c_{66}/(c_{66} \cos^2 \varphi + c_{55} \sin^2 \varphi) \quad (3.5a)$$



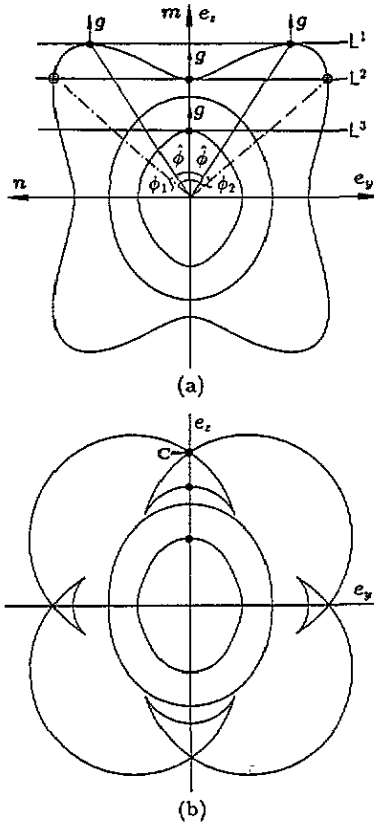


**Figure 2.** Slowness surface and its associated inverse ray surface in the symmetry (100) plane of an orthotropic media: (a) three sheets of slowness surface and group velocities along the symmetry axis, together with the tangent line marked by  $L^{1,2,3}$ ; (b) resultant three sheets of inverse ray surface with respect to the plane. The middle sheet is the elliptic sheet and the inner and outer sheets are the non-elliptic sheets.

which is consistent with the result of Musgrave [1] ((8.2.2b) or (9.3.6)) and Chadwick [15] (8.7). It also shows that both the elliptic slowness surface and its associated inverse ray surface  $v_g^{-1}(\varphi)$  form ellipses. The inclination angle  $\hat{\phi}$  will be given by

$$\hat{p} = \tan \hat{\phi} = -b/(2a) = \Delta_{65} \cos \varphi \sin \varphi / (c_{66} \cos^2 \varphi + c_{55} \sin^2 \varphi) \quad (3.5b)$$

which is consistent with the results of Musgrave [1] (equation (8.2.4)). The equations (3.5) describe the group velocity and the inclination angle for the entire transverse elliptic sheet.

Particularly, along  $e_z$  ( $\varphi = 0^\circ$ ) and  $e_y$  ( $\varphi = 90^\circ$ ) axes, we have two pure modes with group velocities

$$\rho v_{[001](100)}^2 = c_{55} \quad \rho v_{[010](100)}^2 = c_{66} \quad \hat{p} = \tan \hat{\phi} = 0 \quad (3.6)$$

and it is also readily seen that when  $\Delta_{65} = 0$  ( $c_{55} = c_{66}$ ), the slowness surface and the ray surface for the elliptic slowness sheet will become identical circles and the waves of the entire sheet will be pure modes, that is,  $\hat{\phi} = 0$  (figure 2(b)). The group velocity is a single-valued function of ray direction  $m$  and this is a one-to-one correspondence between the slowness surface and the ray surface. When the two elastic constants (diagonal element  $c_{\alpha\alpha}$ ) are equal, both slowness surface and ray surface will become circles and the

waves of the entire sheet will be pure modes. Regarding the recovery of elastic constants, the group velocity measurements in the vicinity of the symmetry axis, say, [001], with respect to the plane, will yield results for both elastic constants. Namely, for  $\varphi = 0^\circ$  one gets  $\rho v^2(0^\circ) = c_{55}$ , and in its neighbourhood,  $\varphi \neq 0^\circ$ , the group velocity  $v(\varphi)$  will give  $c_{66} = c_{55}\rho v^2(\varphi) \sin^2 \varphi / (c_{55} - \rho v^2(\varphi) \cos^2 \varphi)$  according to (3.5a).

*3.1.2. Group velocity related to the in-plane non-elliptic sheets.* For the two in-plane non-elliptic sheets, the Stroh eigenvalues are determined by  $F_2(p, v, \varphi) = 0$  according to (3.3c) which is a fourth-order equation of  $p$ . The degenerate real eigenvalues can be traced by increasing the velocity  $v$ , and it is almost impossible to obtain an analytical expression of the group velocity for the entire sheet. Under the presence of a concavity in the slowness surface, the ray surfaces related to these two sheets may have up to eight degree of freedom because for a straight line there are at most eight intersections over these two ray surfaces. (In the three-dimensional case, it should be  $4 \times 3^2 = 36$  [5].) But, we can at least examine the group velocity along the symmetry direction, along the  $e_z$  axis ( $\varphi = 0^\circ$ ) and the  $e_y$  axis ( $\varphi = 90^\circ$ ), respectively.

*Group velocities along [001](100) direction.* From (3.2) and (3.3c), setting  $\varphi = 0^\circ$ , we get

$$F_2(p, v, 0^\circ) = (c_{44} + p^2 c_{22} - \rho v^2)(c_{33} + p^2 c_{44} - \rho v^2) - p^2 d_1^2 = 0 \quad (3.7)$$

and it can be rewritten as

$$\begin{aligned} F_2(p, v, 0^\circ) &= c_{22}c_{44}p^4 + [c_{22}(c_{33} - \rho v^2) + c_{44}(c_{44} - \rho v^2) - d_1^2]p^2 \\ &\quad + (c_{33} - \rho v^2)(c_{44} - \rho v^2) \\ &= Ap^4 + Bp^2 + C = 0. \end{aligned} \quad (3.8)$$

When  $\rho v^2 \neq c_{33}$  and  $\rho v^2 \neq c_{44}$ , the two pairs of the Stroh eigenvalues must satisfy the expression

$$p^2(v) = [-B \pm (B^2 - 4AC)^{1/2}] / (2A) \quad (3.9)$$

and then the condition for degeneracy must be  $B^2 - 4AC = 0$ . Thus

$$\begin{cases} B^2 - 4AC = G_1 = 0 \\ \hat{p}^2 = \tan^2 \hat{\varphi} = -B / (2A) = G_2 \\ \hat{p}^4 - C/A = \tan^4 \hat{\varphi} - C/A = G_3 = 0. \end{cases} \quad (3.10)$$

The first relation  $G_1 = 0$  in (3.10) yields the equation

$$[c_{22}(c_{33} - \rho v^2) + c_{44}(c_{44} - \rho v^2) - (c_{44} + c_{23})^2]^2 = 4c_{22}c_{44}(c_{33} - \rho v^2)(c_{44} - \rho v^2). \quad (3.11a)$$

We denote the velocity determined by (3.11a)  $v_0$ . This velocity is the group velocity associated with the cuspidal points C in the outermost double tangent parallel to the  $e_y$  axis, like the case shown by line L<sup>1</sup> in figure 2.

We also notice that by setting  $B = 0$  we get  $\rho v^2 = (c_{22}c_{33} + c_{44}^2 - d^2) / (c_{22} + c_{44})$  which is identical to the results of Musgrave (p 103 [1]). But such a situation could not ensure the presence of degeneracy (since  $p^4 = -C/A$ ) and thus the result from  $B = 0$  will not yield group velocity for the cuspidal point C.

The second relation in (3.10)  $G_2$  gives

$$\hat{p}^2 = \tan^2 \hat{\varphi} = [(c_{44} + c_{23})^2 - c_{22}(c_{33} - \rho v_0^2) - c_{44}(c_{44} - \rho v_0^2)] / (2c_{22}c_{44}) \quad (3.11b)$$

which describes the inclination angle between the wave-vector  $k$  and the ray-vector  $g$ .

The third relation in (3.10)  $G_3 = 0$  gives

$$c_{22}c_{44} \tan^4 \hat{\phi} = (c_{33} - \rho v_0^2)(c_{44} - \rho v_0^2) \quad (3.11c)$$

which indicates the simple relation between the group velocity  $v_0$  and the inclination angle  $\hat{\phi}$ . The three relations obtained from the condition of degeneracy (3.10) define both the group velocity and the inclination angle for the cuspidal point.

The remaining situations are related to the case  $C = 0$  in (3.8), which implies that there exist degenerate eigenvalues  $p^2 = 0$ . These cases give pure mode solutions and the group velocities for the pure modes are given by  $\rho v^2 = c_{33}, c_{44}$ . Suppose  $c_{33} > c_{44}$ , the group velocity for the pure mode associated with the outer slowness sheet will be

$$\rho v^2 = c_{44} \quad (3.12)$$

and thus, from (3.8),

$$F_2(p, v, 0^\circ) = c_{44}c_{22}p^4 + [c_{22}(c_{33} - c_{44}) - (c_{44} + c_{23})^2]p^2 = 0 \quad (3.13)$$

which means the group velocity defined by (3.12) is associated with degeneracy for  $\hat{p}^2 = 0$ . The two remaining non-degenerate eigenvalues will be

$$\hat{p} = \pm \{[(c_{44} + c_{23})^2 - c_{22}(c_{33} - c_{44})]/(c_{44}c_{22})\}^{1/2}. \quad (3.14)$$

If the eigenvalues from (3.14) are real, then two bulk wave solutions, as indicated by open circles in figure 2(a) associated with  $p_1 = p_+ = \tan \phi_1$  and  $p_2 = p_- = \tan \phi_2$ , will suggest that the outer slowness sheet must be concave (see also line  $L^2$  in figure 2(a)). If, on the other hand,  $p$  is complex, the outer slowness sheet will be convex. Thus, a condition for the concavity is

$$(c_{44} + c_{23})^2 > c_{22}(c_{33} - c_{44}) \quad (3.15)$$

which is consistent with (3.11b) and agrees with the results of Musgrave ((8.3.4) in [1]). For the pure mode associated with the inner slowness sheet (see line  $L^3$  in figure 2), the group velocity is given by

$$\rho v^2 = c_{33} \quad (3.16)$$

and from (3.8),

$$F_2(p, v, \varphi) = c_{44}c_{11}p^4 + [c_{44}(c_{44} - \rho v^2) - (c_{44} + c_{23})^2]p^2 = 0 \quad (3.17)$$

which again means the group velocity defined by (3.16) is associated with degeneracy  $p = 0$ . The two remaining non-degenerate eigenvalues will be necessarily real because  $\Delta_{34} > 0$  and

$$p = \pm \{[(c_{44} + c_{23})^2 + c_{44}(c_{33} - c_{44})]/(c_{11}c_{44})\}^{1/2}. \quad (3.18)$$

Similarly, when  $c_{44} > c_{33}$ , we will get the condition for the concavity as

$$(c_{44} + c_{23})^2 > c_{44}(c_{44} - c_{33}) \quad (3.19)$$

which is easy to prove.

In the above analysis, many characteristic points in the ray surface have been identified in the presence of an axial concave region in the slowness surface. These points are the pure mode points, the cuspidal point and the entire transverse elliptic sheet. From group velocities related to these characteristic points we can determine virtually all six elastic constants involved in the plane. To be explicit, along a symmetry axis, we can always obtain three diagonal elements  $c_{\sigma\sigma}$  from pure mode measurements, among which are one normal and two shear stiffness constants. The measurement of group velocities for the transversely polarized elliptic sheet will determine another diagonal shear constant  $c_{\sigma\sigma}$ . Subsequently, the

group velocity  $v_0$  for the cuspidal point itself alone can provide a relation (3.11a) between the remaining diagonal element  $c_{\sigma\sigma}$  and the only off-diagonal element  $c_{\sigma\delta}$  ( $c_{22}$  and  $c_{23}$  in the (100) plane case). This relation is one of the most important ones we have obtained so far. For the cuspidal point, if we can determine the inclination angle  $\hat{\phi}$  experimentally, (3.11c) will give the remaining diagonal element  $c_{\sigma\sigma}$  (here  $c_{22}$ ) and thus (3.11a) determines the off-diagonal element  $c_{\sigma\delta}$  uniquely. Of course, all the diagonal elements  $c_{\sigma\sigma}$  can be determined from pure modes and thus utilizing (3.11a) the determination of off-diagonal elements also becomes possible. In summary, for group velocities for the [001](100) case, we have

$$\rho v_{[001](100)}^2 = [c_{33}, c_{44}, c_{55}]_{\text{pure mode}}, [c_{66}]_{\text{ellips. sheet}}, [\rho v_0^2(c_{23}), c_{22}(\hat{\phi})]_{\text{cusp}} \quad (3.20)$$

where the first three diagonal elements  $c_{\sigma\sigma}$  are associated with group velocities of the pure modes,  $c_{66}$  pertains to the transverse elliptic sheet and  $c_{23}$  and  $c_{22}$  are related to the cuspidal point. It is clear that all six elastic constants involved in the (100) plane can be recovered from group velocities and inclination angle with respect to the plane.

*Group velocities along [010](100) direction.* For the group velocities along the  $e_y$  direction, by setting  $\varphi = 90^\circ$ , the analysis is similar to that for the  $e_z$  direction in the (100) plane. Similarly to the equations (3.11), (3.12), (3.15), (3.16), (3.19), we get for the cusp

$$[c_{33}(c_{22} - \rho v_0^2) + c_{44}(c_{44} - \rho v_0^2) - (c_{44} + c_{23})^2]^2 = 4c_{33}c_{44}(c_{22} - \rho v_0^2)(c_{44} - \rho v_0^2) \\ \hat{\rho}^2 = \tan^2 \phi = [(c_{44} + c_{23})^2 - c_{33}(c_{22} - \rho v_0^2) - c_{44}(c_{44} - \rho v_0^2)] / (2c_{33}c_{44}) \quad (3.21)$$

$$c_{33}c_{44} \tan^4 \hat{\phi} = (c_{22} - \rho v_0^2)(c_{44} - \rho v_0^2)$$

and for the pure modes

$$\rho v_{[010](100)}^2 = c_{22}, \quad \rho v_{[010](100)}^2 = c_{44} \quad (3.22)$$

while for the concavity

$$(c_{44} + c_{23})^2 > c_{33}(c_{22} - c_{44}) \quad \text{when } c_{22} > c_{44} \\ (c_{44} + c_{23})^2 > c_{44}(c_{44} - c_{22}) \quad \text{when } c_{44} > c_{22}. \quad (3.23)$$

and the group velocities along the direction will be

$$\rho v_{[010](100)}^2 = [c_{22}, c_{44}, c_{66}]_{\text{pure mode}}, [c_{55}]_{\text{ellips. sheet}}, [\rho v_0^2(c_{23}), c_{33}(\hat{\phi})]_{\text{cusp}}. \quad (3.24)$$

The advantage of the  $e_y$  direction is that the propagation along this direction will remain non-degenerate for the tetragonal and transversely isotropic media.

The above is just the result for symmetry directions [001] and [010] with respect to (100) symmetry plane. Similarly we can find group velocities for other symmetric directions with respect to the two main symmetry planes in orthotropic media, namely, [001](010), [100](010), [100](001), [010](001). Here we just sum up all the final results for further discussion.

$$\rho v_{[001](100)}^2 = [c_{33}, c_{44}, c_{55}]_{\text{pure mode}}, [c_{66}]_{\text{ellips. sheet}}, [\rho v_0^2(c_{23}), c_{22}(\hat{\phi})]_{\text{cusp}} \quad (3.25)$$

$$\rho v_{[010](100)}^2 = [c_{22}, c_{44}, c_{66}]_{\text{pure mode}}, [c_{55}]_{\text{ellips. sheet}}, [\rho v_0^2(c_{23}), c_{33}(\hat{\phi})]_{\text{cusp}} \quad (3.26)$$

$$\rho v_{[001](010)}^2 = [c_{33}, c_{55}, c_{44}]_{\text{pure mode}}, [c_{66}]_{\text{ellips. sheet}}, [\rho v_0^2(c_{13}), c_{11}(\hat{\phi})]_{\text{cusp}} \quad (3.27)$$

$$\rho v_{[100](010)}^2 = [c_{11}, c_{55}, c_{66}]_{\text{pure mode}}, [c_{44}]_{\text{ellips. sheet}}, [\rho v_0^2(c_{13}), c_{33}(\hat{\phi})]_{\text{cusp}} \quad (3.28)$$

$$\rho v_{[010](001)}^2 = [c_{22}, c_{66}, c_{44}]_{\text{pure mode}}, [c_{55}]_{\text{ellips. sheet}}, [\rho v_0^2(c_{12}), c_{11}(\hat{\phi})]_{\text{cusp}} \quad (3.29)$$

$$\rho v_{[100](001)}^2 = [c_{11}, c_{66}, c_{55}]_{\text{pure mode}}, [c_{44}]_{\text{ellips. sheet}}, [\rho v_0^2(c_{12}), c_{22}(\hat{\phi})]_{\text{cusp}}. \quad (3.30)$$

The essence of the present analysis is the degeneracy in the Stroh eigenvalue equation, and we call such a scheme the *degeneracy analysis approach* (DAA). As for the inverse problem, the relations we have established so far provide us with an effective and practical tool to recover the elastic constants. One can observe that, under certain circumstances (for example, when there exist axial concavities along the [001] direction with respect to (100) and (010) planes), the group velocities and the inclination angles for a single direction enable us to determine up to eight elastic constants among nine independent constants. All nine elastic constants for orthotropic media can be recovered from group velocity measurements for *two* symmetry directions if there are some axial concavities present and both the group velocities  $v_0$  and the inclination angles  $\hat{\phi}$  for cuspidal points can be determined. In the cases where there is no axial concavity at all, which is very likely, group velocities for all three directions could only provide enough relations for recovering all the diagonal elements. We will show in the next subsection that the remaining off-diagonal elements can be recovered from group velocities along the directions in the neighbourhood of the symmetry directions.

### 3.2. Off-symmetric cases: numerical implementation

There are some cases that have not been mentioned in the earlier discussion, namely, the group velocities associated with off-symmetry directions and concavities centred at off-symmetry directions. In these cases, the main concern is to determine off-diagonal elements related to the two non-elliptic sheets. Therefore, we now return to the general discussion in section 2 and resume degeneracy analysis in an arbitrary ray direction  $\varphi$  in a symmetry plane. This is particularly important to the cases when there is no axial concavity exists along the symmetry direction.

Now we re-examine equation (3.3) for the in-plane non-elliptic sheets. The polynomial  $F_2 = F_2(p, v, \varphi, c_{\sigma\sigma}, c_{\sigma\delta})$ , for a given measured group velocity  $v$  along an arbitrary direction  $\hat{\phi}$  and with all  $c_{\sigma\sigma}$  known, will become a very simple fourth-order polynomial of  $p$  with coefficient as functions of an off-diagonal element  $c_{\sigma\delta}$ . Then  $c_{\sigma\delta}$  must be such that the equation  $F_2(p, c_{\sigma\delta}) = 0$  does yield at least one pair of degenerate roots.

The most essential feature for the ray surface is that the group velocity is related to a degenerate solution of the Stroh eigenvalue equation. Notice that an imaginary root ( $p$ ) represents an evanescent wave, a real root ( $p = \tan \phi$ ) represents a bulk wave and a pair of real degenerate roots ( $\hat{p} = \tan \hat{\phi}$ ) represents a bulk wave solution for the group velocity. Since the group velocity may be associated with various types of envelope construction as indicated in figure 3, where only two in-plane non-elliptic sheets are illustrated, we will categorize the various possible cases which are physically significant to the inverse problem.

We first investigate the group velocities related to the outer in-plane non-elliptic sheet.

(1) Symmetric concavity:  $F_2(p, c_{\sigma\delta}) = (a_1 p^2 + c_1)^2 = 0$  with two pairs of degenerate real eigenvalues, identical but opposite in sign, such that  $p_1 = p_2 = \tan \phi_1$  and  $p_3 = p_4 = -\tan \phi_1$ . This is related to a symmetric concavity where a double tangent with equal inclination angles can be constructed. (See line  $L_1$  in figure 3.)

(2) Asymmetric concavity:  $F_2(p, c_{\sigma\delta}) = (a_1 p^2 + b_1 p + c_1)^2 = 0$  with two pairs of degenerate real eigenvalues, such that  $p_1 = p_2 = \tan \phi_1$  and  $p_3 = p_4 = \tan \phi_2$ . This is

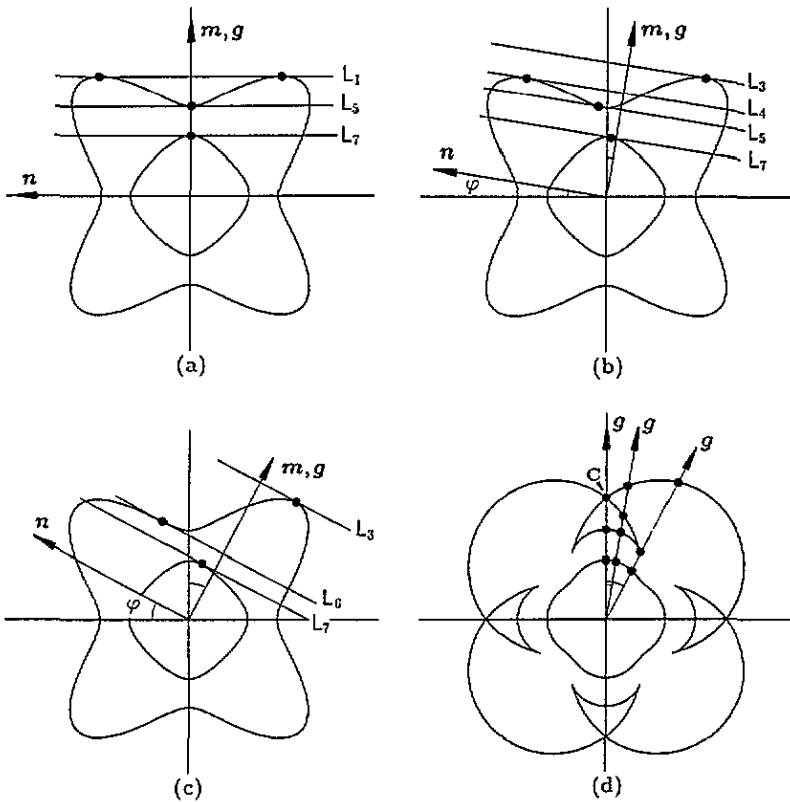


**Figure 3.** Geometric interpretation of various pedal constructions with respect to a symmetry plane and the group velocities related to the non-elliptic slowness sheets (here only these two sheets are drawn): (a)–(c) group velocities for symmetric and asymmetric directions; (d) the resultant inverse ray surface. Various lines  $L$  represent the relationship between different group velocities and their phase velocities, and the filled circles represent the bulk wave solutions associated with a given ray-vector  $g$ .

related to an asymmetric concavity where a double tangent with different inclination angles can be constructed.

(3) Convex case:  $F_2(p, c_{\sigma\delta}) = (a_1 p + c_1)^2(a_2 p^2 + b_2 p + c_2) = 0$  with one pair of degenerate real eigenvalues and one pair of non-degenerate complex conjugate eigenvalues. This is associated with the group velocity related to the outermost part of a concavity. This is also valid for the case when there is no concavity in the slowness surface. (See line  $L_3$  in figure 3.)

(4) Convex case:  $F_2(p, c_{\sigma\delta}) = (a_1 p + c_1)^2(a_2 p^2 + b_2 p + c_2) = 0$  with one pair of degenerate real eigenvalues and one pair of non-degenerate real eigenvalues. This is associated with the group velocity related to the inner convex part of a concavity. (See line  $L_4$  in figure 3.)

(5) Concave case:  $F_2(p, c_{\sigma\delta}) = (a_1 p + c_1)^2(a_2 p^2 + b_2 p + c_2) = 0$  with one pair of degenerate real eigenvalues and one pair of non-degenerate real eigenvalues. This is associated with the group velocity related to the inner concave part of a concavity. (See line  $L_5$  in figure 3.)

(6) Cuspidal tip case:  $F_2(p, c_{\sigma\delta}) = (a_1 p + c_1)^3(a_2 p + c_2) = 0$  with three identical real eigenvalues (triplicate degeneracy), and one real eigenvalue, say,  $p_1 = p_2 = p_3 = \tan \phi_1$

and  $p_4 = \tan \phi_2$ . It is associated with an inflectional zero-curvature point of a concavity. (See line  $L_6$  in figure 3.)

For the group velocities related to the inner in-plane non-elliptic sheet, since it is globally convex everywhere, we have only one case for this sheet.

(7) Convex case:  $F_2(p, c_{\sigma\delta}) = (a_1 p + c_1)^2 (a_2 p^2 + b_2 p + c_2) = 0$  with one pair of degenerate real eigenvalues and one pair of non-degenerate real eigenvalues. (See line  $L_7$  in figure 3.) The group velocity related to the inner slowness sheet is important for experimental convenience because of the higher accuracy in the determination of group velocities for fast waves.

In all cases, for a given direction  $\varphi$  and a given (measured) group velocity  $v_g$  with respect to a symmetry plane, with all the diagonal elements  $c_{\sigma\sigma}$  known from pure mode measurements, we can determine the remaining off-diagonal element  $c_{\sigma\delta}$ , which is related solely to the in-plane non-elliptic sheets, by numerical substitution of  $c_{\sigma\delta}$  so that the condition for the relevant situation of the situations (1)–(7) is satisfied at the the point  $(v_g, \varphi)$  of interest. Eventually, we will have recovered all elastic constants involved in a symmetry plane even without presence of an axial concavity, and further all nine elastic constants of orthotropic media.

Of course, one can determine the remaining off-diagonal element by solving the Stroh eigenvalue equation numerically when all the diagonal elements are known. But explicit formulation of  $F_2$  has an advantage even when one has one diagonal element unknown. We can still find out certain useful relations by constructing the resultant polynomial from two  $F_2$  related to two angles or two sheets or a relation like (3.11a). We will not pursue such a special scheme further here.

Here we can consider a simple case. In the (100) plane, we assume the group velocities along an angle  $\varphi_i$  are  $v_1$  and  $v_2$  and related to an outer and inner slowness surface, respectively, which are both globally convex. When all diagonal elements  $c_{\sigma\sigma}$  are known from pure mode measurements, we will have  $F_2 = F_2(v_1, p, c_{23}) = 0$  and  $F_2 = F_2(v_2, p, c_{23}) = 0$  for  $v_1$  and  $v_2$  respectively. According to the above analysis, case (3) and case (7),  $F_2(v_1, p, c_{23}) = 0$  should yield one pair of real eigenvalues and one pair of non-degenerate complex conjugate eigenvalues, and  $F_2 = F_2(v_2, p, c_{23}) = 0$  should yield one pair of real eigenvalues and one one pair of non-degenerate real eigenvalues, respectively. By numerical substitution of  $c_{23}$ , we can have it uniquely determined, and the results for  $c_{23}$  obtained from these two group velocities should be identical. Of course, the eventual estimate for  $c_{23}$  can be further calibrated by scanning over more data points from group velocity measurements.

Apart from the inverse problem, the DAA can also be adopted as a practical scheme for locating the pure mode direction for which  $\hat{p} = \tan \hat{\phi} = 0$  and  $\hat{p}^{2n} = 0$  (where  $n = 1, 2, 3$ ), and the exponent  $n$  represents the multiplicity of the pure mode. For example, when  $\rho v^2 = c_{44}$ , the [001] direction in the (100) plane in tetragonal media is a pure mode direction where  $\hat{p}^4 = 0$  and such a multiply degenerate solution for the group velocity is related to both the outer sheet and the elliptic sheet.

#### 4. Illustrative examples

We now demonstrate two examples of application of DAA scheme to two orthotropic media:  $\alpha$ -uranium and oak [1]. In tables 1 and 2, we list some details of the inverse scheme for recovering elastic constants from group velocities and inclination angles. We start with

a set of elastic constants and calculate the slowness surface, ray surface and inclination angles, and set numerical data for group velocity and inclination angles into the relations we established in section 3 and have the elastic constants recovered.

For  $\alpha$ -uranium (see table 1), there exist two axial concavities along [001](100) and [010](100) and one non-symmetric concavity in the (010) plane (see figures 9.31–9.33 in [1]). The nine elastic constants can be recovered by measuring the group velocity in all three main symmetry directions, although there are axial concavities present in the slowness surface.

Along the [001](100) direction and its vicinity (see the first column of table 1), one can completely determine six elastic constants from the pure modes, transverse sheet and cuspidal point. The numerical scheme is also tested to recover  $c_{23}$  when  $c_{22}$  is known beforehand. The same applies to the [010](100) direction (see the third column of table 1). The other columns show results for the remaining four cases. One should notice that certain diagonal constants  $c_{\sigma\sigma}$  must be given so that the numerical calculation of the off-diagonal constant  $c_{\sigma\delta}$  can be determined when there is no axial concavity, such as the case in the [010](100) direction (see the second column of table 1). For this reason, in the table we made some remarks on a certain direction along which a complete (or incomplete) recovery is possible and therefore it is the most preferred direction (with two asterisks).

**Table 1.** Orthotropic  $\alpha$ -uranium:  $c_{11} = 21.5$ ,  $c_{22} = 19.9$ ,  $c_{33} = 26.7$ ,  $c_{44} = 12.4$ ,  $c_{55} = 7.30$ ,  $c_{66} = 7.40$ ,  $c_{12} = 4.60$ ,  $c_{13} = 2.20$ ,  $c_{23} = 10.7$ .

|               | [001]   |   | [010]  |   | [100]   |   |
|---------------|---|---|--|---|---|---|
|               | (100)   | (010)   | (100)  | (001)   | (010)   | (001)   |
| Pure mode     | $c_{33} = 26.7$<br>$c_{44} = 12.4$<br>$c_{55} = 7.30$                                   | $c_{33} = 26.7$<br>$c_{44} = 12.4$<br>$c_{55} = 7.30$                         | $c_{22} = 19.9$<br>$c_{44} = 12.4$<br>$c_{66} = 7.40$                            | $c_{22} = 19.9$<br>$c_{44} = 12.4$<br>$c_{66} = 7.40$                         | $c_{11} = 21.5$<br>$c_{55} = 7.30$<br>$c_{66} = 7.40$                         | $c_{11} = 21.5$<br>$c_{55} = 7.30$<br>$c_{66} = 7.40$                         |
| Ellips. sheet | $c_{66} = 7.40$   | $c_{66} = 7.40$   | $c_{55} = 7.30$  | $c_{55} = 7.30$   | $c_{44} = 12.4$   | $c_{44} = 12.4$   |
| Cusp. point   | $\rho v_0^2 = 10.34$<br>$\hat{\phi} = 31.3^\circ$<br>$c_{23} = 10.7$<br>$c_{22} = 19.9$ |   | $\rho v_0^2 = 9.26$<br>$\hat{\phi} = 29.4$<br>$c_{23} = 10.7$<br>$c_{33} = 26.7$ |   |   |   |
| Num. calc.    | $\rho v^2 = 27.07$<br>$\varphi = 10.0^\circ$<br>$c_{23} = 10.7$<br>Complete             | $\rho v^2 = 25.79$<br>$\varphi = 10.0^\circ$<br>$c_{13} = 2.20$<br>Incomplete | $\rho v^2 = 12.90$<br>$\varphi = 10.0^\circ$<br>$c_{23} = 10.7$<br>Complete      | $\rho v^2 = 19.87$<br>$\varphi = 10.0^\circ$<br>$c_{12} = 4.60$<br>Incomplete | $\rho v^2 = 21.16$<br>$\varphi = 10.0^\circ$<br>$c_{13} = 2.20$<br>Incomplete | $\rho v^2 = 21.36$<br>$\varphi = 10.0^\circ$<br>$c_{12} = 4.60$<br>Incomplete |
| Pref. dir.    | **  | *   | **   | *   |   |   |

The example of oak, also an orthotropic medium (see table 2), has two axial concavities along [001] and [010] with respect to the (100) plane and two axial concavities along [100] and [010] with respect to the (001) plane. Table 2 (see the third and fourth columns of table 2) shows that the group velocities for the [010] direction can give eight elastic constants leaving only  $c_{13}$  undetermined. The constant  $c_{13}$  can be determined subsequently from, for example, the vicinity of [001](010) direction. We also notice that  $c_{23}$  and  $c_{12}$  are the same in value, but this does not necessarily mean that group velocities for the cuspidal points in the two planes are identical since  $c_{33}$  and  $c_{11}$  are different. This can also be observed in the point source case in the [010] direction.

However, if the inclination angle  $\hat{\phi}$  for the cuspidal point cannot be determined, the relevant diagonal constant must be determined from measurements in all three symmetry



**Table 2.** Orthotropic oak:  $c_{11} = 0.305$ ,  $c_{22} = 0.138$ ,  $c_{33} = 0.682$ ,  $c_{44} = 0.780$ ,  $c_{55} = 0.132$ ,  $c_{66} = 0.400$ ,  $c_{12} = 0.103$ ,  $c_{13} = 0.150$ ,  $c_{23} = 0.103$ .

|              | [001]   |   | [010]   |   | [100]  |  |
|--------------|---|---|---|---|--|--|
|              | (100)   | (010)   | (100)   | (001)   | (010)  | (001)  |
| Pure mode    | $c_{33} = 0.682$<br>$c_{44} = 0.780$<br>$c_{55} = 0.132$                                  | $c_{33} = 0.682$<br>$c_{44} = 0.780$<br>$c_{55} = 0.132$                                  | $c_{22} = 0.138$<br>$c_{44} = 0.780$<br>$c_{66} = 0.400$                                  | $c_{22} = 0.138$<br>$c_{44} = 0.780$<br>$c_{66} = 0.400$                                  | $c_{11} = 0.305$<br>$c_{55} = 0.132$<br>$c_{66} = 0.400$                       | $c_{11} = 0.305$<br>$c_{55} = 0.132$<br>$c_{66} = 0.400$                     |
| Ellips sheet | $c_{66} = 0.400$  | $c_{66} = 0.400$  | $c_{55} = 0.132$  | $c_{55} = 0.132$  | $c_{44} = 0.780$   | $c_{55} = 0.780$   |
| Cusp. point  | $\rho v_0^2 = 0.255$<br>$\hat{\phi} = 50.2^\circ$<br>$c_{23} = 0.103$<br>$c_{22} = 0.138$ | $\rho v_0^2 = 0.102$<br>$\hat{\phi} = 24.8^\circ$<br>$c_{23} = 0.103$<br>$c_{33} = 0.682$ | $\rho v_0^2 = 0.073$<br>$\hat{\phi} = 32.9^\circ$<br>$c_{12} = 0.103$<br>$c_{11} = 0.305$ | $\rho v_0^2 = 0.111$<br>$\hat{\phi} = 45.1^\circ$<br>$c_{12} = 0.103$<br>$c_{22} = 0.138$ |  |  |
| Num. calc.   | $\rho v^2 = 0.705$<br>$\varphi = 10.0^\circ$<br>$c_{23} = 1.03$<br>Complete               | $\rho v^2 = 0.653$<br>$\varphi = 10.0^\circ$<br>$c_{13} = 0.150$<br>Incomplete            | $\rho v^2 = 0.794$<br>$\varphi = 10.0^\circ$<br>$c_{23} = 0.103$<br>Complete              | $\rho v^2 = 0.408$<br>$\varphi = 10.0^\circ$<br>$c_{12} = 0.103$<br>Complete              | $\rho v^2 = 0.310$<br>$\varphi = 10.0^\circ$<br>$c_{13} = 0.150$<br>Incomplete | $\rho v^2 = 0.411$<br>$\varphi = 10.0^\circ$<br>$c_{12} = 0.103$<br>Complete |
| Pref. dir.   |   | *   | **  | **  |  |  |

directions, and then the off-diagonal elements can be determined afterwards. For example, one can determine all the diagonal elements from pure modes along all three directions and afterwards recover off-diagonal elements from numerical calculation in the vicinity of symmetry directions.

### 5. Discussions

The DAA provides a direct scheme to determine group velocities together with inclination angles as well as an inversion procedure for recovering elastic constants of anisotropic media. But it has also a minor disadvantage, namely, the high number of degrees of freedom of the ray surface (which may be up to eight for the ray surface for two non-elliptic sheets in the two-dimensional case considered) prevents us from obtaining general explicit expressions for the group velocity and the inclination angle for an arbitrary direction in a symmetry plane.

For elastic media with higher elastic symmetry, such as tetragonal, transversely isotropic, cubic and isotropic media, the DAA can be readily applied. However, one has to do the analysis in other symmetry directions and symmetry planes, such as  $\langle 110 \rangle$  directions and  $\{110\}$  planes. Thus is because the independent elastic constants in these media are fewer with increasing symmetry and the symmetry directions/planes we considered become equivalent. So far, we have considered most of the low-index symmetry (or pure mode) directions and symmetry planes in the media with higher elastic symmetry (to be presented elsewhere).

Concerning the application of the DAA to practical inversion, we make the following comments on the relationship between the present formalism and experimental realizations.

- (1) In the line source cases to which DAA applies, recovery of elastic constants from group velocity data of one symmetry plane can be carried out in three steps: (i) group velocities for pure modes give at most three diagonal elements; (ii) the ray surface for the elliptic sheet will give another diagonal element; (iii) the group velocity and its associated inclination angle for the cuspidal point will determine one more diagonal element and one off-diagonal element, and even if the inclination angle is not available, the off-diagonal

element can still be recovered when all the diagonal elements are determined from pure mode measurements for other directions; (iv) after we run through all the main symmetry planes and symmetry directions we can have all the diagonal elements recovered together with the off-diagonal elements related to axial concavities when they exist.

In some cases, the procedure becomes very simple. In cubic media, for example, a *single* measurement along a symmetry axis [001], when there is an axial concavity, will determine *all* three elastic constants.

(2) The presentation of DAA is mainly for the two-dimensional system, and we have assumed that the line source lies normal to the symmetric reference plane ( $m, n$ ). Therefore, the group velocity for the cuspidal point is dependent on the plane in which the inclination angle is defined. However, the validity of the DAA results still holds for the point source situation. The reason is that the group velocities obtained for the symmetry plane are embedded in the ray surface. In other words, the ray surface constructed from tangent planes for the three-dimensional case will include the ray surface obtained from the two-dimensional pedal construction. The ray surface for the three-dimensional case may include more branches than that for the two-dimensional case when there is a concavity in the slowness surface. Physically, the group velocity and energy flux for the bulk wave propagating in the symmetry plane will be confined within the symmetry plane and the ray surface thus will be identical to the sheet for the three-dimensional situation.

Application of a point source has the advantage that it is efficient for group velocity measurements when there are axial concavities present. For example, if the two  $v_0$  for the cuspidal points [001](100) and [001](010) are different (since the three-dimensional ray surface will be multivalued) the two  $v_0$  can be determined from a single measurement along [001]. On the other hand, a disadvantage is the complexity of the ray surface in off-symmetry directions. This causes difficulties in accurate measurements of group velocities for slow waves (related to the outer non-elliptic sheet) even along pure mode directions and, sometimes, only the group velocity for fast waves (related to the inner non-elliptic sheet) can be recorded accurately.

## 6. Conclusions

The characteristic surfaces for acoustic bulk wave propagation in anisotropic media, the slowness surface and the ray surface, are investigated in terms of the Stroh formalism for two-dimensional elastodynamics. By examining the degeneracy of the Stroh eigenvalue equation, the degeneracy analysis approach (DAA) for the construction of the ray surface is established. The main advantage of DAA is that it gives both the group velocity and the bulk wave inclination angle for a given direction.

The present investigation focuses on explicit mathematical relations between the ray surface and elastic constants for some symmetry directions with respect to symmetry planes. In symmetry planes, the group velocity and inclination angle for the elliptic slowness sheet (related to out-of-plane transversely polarized waves) can be derived explicitly for the entire sheet. In the presence of axial concavity in the outer non-elliptic slowness sheet in the symmetry planes, there will be cuspidal points in the ray surface, and application of DAA to the cuspidal point and the pure modes can recover eventually all the elastic constants of media with orthotropic (and higher) elastic symmetry. The analytical relations between group velocities and elastic constants for orthotropic media are verified by illustrative examples.

Although analytical results are obtained only for some symmetry directions, a practical numerical scheme for off-symmetry directions is presented complementarily, which enables

us to deduce some off-diagonal elastic constants under certain circumstances. For practical applications, the relation between the line source case and point source case is particularly important. We expect that the present formalism can be adopted in the general discussion of ray surfaces in the three-dimensional case, and especially for the media with high elastic symmetry.

### Acknowledgments

The author would like to thank Professor J Lothe and Professor M J P Musgrave for their comments and discussions. Comments from referees are gratefully appreciated.

### References

- [1] Musgrave M J P 1970 *Crystal Acoustics* (San Francisco, CA: Holden-Day)
- [2] Auld B A 1973 *Acoustic Fields and Waves in Solids* (New York: Wiley)
- [3] Cowin S C and Mehrabadi M M 1987 *Q. J. Mech. Appl. Math.* **40** 451
- [4] Van Buskirk W C, Cowin S C and Carter J Jr 1986 *J. Mater. Sci.* **21** 2759
- [5] Musgrave M J P 1994 private communications
- [6] Every A G 1981 *Phys. Rev. B* **24** 3456
- [7] Sachse W and Kim K Y 1987 *Review of Progress in Quantitative Evaluation* vol 6A, ed D O Thompson and D E Chimenti (New York: Plenum) p 311
- [8] Kim K Y, Sachse W and Every A G 1993 *J. Acoust. Soc. Am.* **93** 1393
- [9] Kim K Y and Sachse W 1994 *J. Appl. Phys.* **75** 1435
- [10] Every A G and Sachse W 1990 *Phys. Rev. B* **42** 8196
- [11] Stroh A N 1962 *J. Math. Phys.* **41** 77
- [12] Chadwick P and Smith G D 1977 *Advances in Applied Mechanics* vol 17 (New York: Academic) p 303
- [13] Alshits V I and Lothe J 1979 *Sov. Phys.-Crystallogr.* **24** 387, 393, 644
- [14] Chadwick P and Smith G D 1982 *Mechanics of Solids, the Rodney Hill 60th Anniversary Volume* ed H G Hopkins and M J Sewell (Oxford: Pergamon) p 47
- [15] Chadwick P 1989 *Proc. R. Soc. A* **422** 23
- [16] Alshits V I and Lothe J 1978 *Sov. Phys.-Crystallogr.* **23** 509
- [17] Wang L and Lothe J 1992 *Wave Motion* **16** 89, 101
- [18] Chadwick P 1990 *Proc. R. Soc. A* **430** 231